



Determination of Chrome Deposits by Applying the Cellular Neural Network (CNN) Method to the Gravity Anomaly Map of the Erzincan-Kop Mountain (Turkey) Region

Ali Muhittin Albora

Istanbul University-Cerrahpaşa, Engineering Faculty, Geophysical Department, 2022, Büyükçekmece-Istanbul, Turkey

Email: muhittin@iuc.edu.tr

Abstract In this study, the Gravity Anomaly map was used in the investigation of Chromium mineral deposits in the Erzincan-Kop Mountain region in Turkey. Cellular Neural Network (CNN) method was applied to the gravity anomaly map and the locations of chrome ore were determined from the obtained CNN map. The aim here is to determine the real locations and properties of the objects at the investigated depth with the least error. In this study, the structures at the depth we want can be de-noised with the CNN method, and it allows us to view the residual structures. The densities of chromium in this region and dunite, which is the country rock in which chromium is found, show slight differences. For this reason, it becomes difficult to determine the locations of the ore on the gravity anomaly map. In order to find these small differences, the residual anomaly map was obtained by applying the CNN method to the residual anomaly map.

Keywords Gravity anomaly map, chrome ore, Cellular Neural Network (CNN), Turkey

Introduction

Chromium (24Cr), as one of the basic elements of the chemical and metal industry, is widely used to prevent corrosion of alloy metals. Chromium forms a thin rusty layer when in contact with oxygen in the air. This thin layer is as thin as a few atoms thick, but because it is very dense, it prevents oxygen from entering the metal part under the layer. The first use of chromium is known in China in the 3rd century BC. In 1762, the German mineralogist and geologist Johann Gottlob Lehmann first discovered chromium-containing minerals in the region of the Ural mountains (Russia). In 1797, Nicolas Louis Vauquelin of France (1763-1829) succeeded in obtaining chromium trioxide (CrO_3) from crocoite (PbCrO_4) and pure chromium from chromium trioxide [1]. Thus, chrome has found widespread use. Chromium is the natural component of the earth's crust and is found in the form of chromite ($\text{FeCr}_2\text{O}_4\text{-MgAl}_2\text{O}_4$), 60% in stratiform-layered chrome deposits and 40% in alpine type chrome deposits. Turkey is one of the 4 countries that produce the most chrome in the world. Turkey's chrome deposits are alpine type chrome deposits. Alpine-type chrome deposits are not like chrome deposits with stratiform layers, which are found in layers that are kilometers long, but are collected together with dunite [1,2]. Gravity anomaly map was obtained in the Erzincan-Kop Mountain region. By applying the CNN algorithm to the gravity anomaly map, the boundaries of the places where the mine is located were determined and the locations of the mine were clearly revealed. The CNN method was used as a separation and boundary detection method, which is an important feature in gravity data. The most important feature of the CNN method is that it takes into account neighborhood relations. HYSA was first introduced by [3]. The CNN method was first applied to Geophysical studies and successful results were obtained [4-5].



Method

Cellular Neural Networks

Cellular neural networks are mostly structures made up of cells arranged to form a two-dimensional array. Contrary to known artificial neural networks, every cell here is in connection with the cells in its close neighborhood (Figure-1).

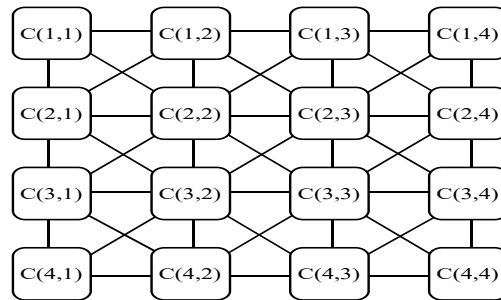


Figure 1: Two-dimensional (4x4) cellular neural network [4]

Each cell in these structures:

- a) A linear input unit with weighted addition
- b) A linear dynamic interface
- c) It is a dynamic circuit consisting of a piece-wise linear (Piece-Wise Linear: PWL) output unit symmetrical with respect to the origin (Figure-2).

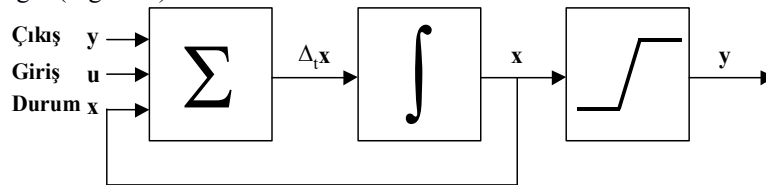


Figure 2: Block diagram of an artificial neural network [4]

The r-neighborhood of a cell in a Cellular Artificial Neural Network (HYSA) is defined as follows.

$$N_r(i, j) = \{C(k, l) | \max(|i - k|, |j - l|) \leq r, \quad 1 \leq i \leq M; 1 \leq j \leq N\} \quad (1)$$

Here:

(i, j) : The index vector that determines the location of the cells in the array,

$C(i, j)$: i. Row, j. It is the parameter that indicates the location of the cell in the column.

The differential equations characterizing the cellular neural network can be written as:

$$\frac{dx_{i,j}(t)}{dt} = -S \cdot x_{i,j}(t) + \sum_{(k,l) \in N(i,j)} A_{i,j;k,l} \cdot y_{k,l}(t) + \sum_{(k,l) \in N(i,j)} B_{i,j;k,l} \cdot u_{k,l}(t) + I_{i,j} \quad (2)$$

$$y_{i,j}(t) = f[x_{i,j}(t)] = \frac{1}{2} \cdot (|x_{i,j}(t) + 1| - |x_{i,j}(t) - 1|) \quad (3)$$

$A_{i,j}$: Feedback link weighting coefficients

$B_{i,j}$: Input connection weight coefficients

I : Threshold level, which is generally the same for each cell

S : State feedback weight coefficient

is defined as.

The equation characterizing the Discrete-Time Cellular Artificial Neural Network is expressed as follows.

$$x_{i,j}(n + 1) = \sum_{(k,l) \in N(i,j)} A_{i,j;k,l} \cdot y_{k,l}(n) + \sum_{(k,l) \in N(i,j)} B_{i,j;k,l} \cdot u_{k,l}(n) + I_{i,j} \quad (4)$$

$$y_{i,j}(n) = f[x_{i,j}(n)] = \frac{1}{2} \cdot (|x_{i,j}(n) + 1| - |x_{i,j}(n) - 1|) \quad (5)$$



It should be noted that in this equation, besides the classical filtering, an iterative filtering from the A feedback link weight coefficients is also performed.

Here, the entries of the cells $u_{i,j}$ are real numbers that take values in the range $[-1,1]$. The outputs of the cells $y_{i,j}$ are the outputs that can only take the values of -1 or $+1$ if the stability conditions are met at the end of a certain time (or cycle) [5].

One of the most important features that distinguishes CNN from known artificial neural networks is that the feedback (A) and input (B) connection weight coefficients form an invariant connection network on the studied plane (Space Invariance Property) (Figure 3).

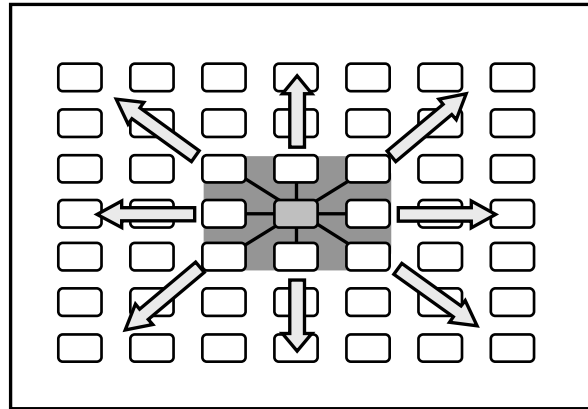


Figure 3: The property of invariance in the plane [4]

$$A(i, j; k, l) = A(k - i, l - j) \quad B(i, j; k, l) = B(k - i, l - j) \quad (6)$$

Work Area

The Erzincan-Kop region, where the North Anatolian Fault passes, one of the two main active faults of Turkey, is the region where various elements and especially the chrome ores of Kop Mountain are found, since it is within the ophiolitic belt (Figure 4). The Merkez, Refahiye, Iliç, Kemah, Tercan and Çayırılı fields of the Erzincan-Kop mountain region are the second important chrome source after the Güleman-Elazığ region. The amount of chromium in the Erzincan-Kop mountain region is known as 3.6 million tons (34-44%) [2].

Geology of the Region

Regional geology In the Erzincan region, there are four basic tectono-stratigraphic units of pre-Eocene age, reflecting different environmental conditions and tectonically related to each other. In the study area, Çimendağı Nappe, Erzincan Nappe and Munzur Limestone representing the southern margin of the Eastern Pontides were identified. The Tertiary-Quaternary cover is located on the tectonic units with an angular unconformity. Çimendağı Napi consists of pre-Liassic metamorphic rocks and Jurassic-Cretaceous aged rocks composed of mainly conglomerate and sandstone, which overlie the granites cutting these rocks with an angular unconformity, and shallow marine at lower levels and pelagic limestones at the upper part. The Erzincan Nappe consists of ophiolite nappes represented mainly by peridotites and olistostromal ophiolite mixed in places. The ophiolites were named Refahiye Complex, and the olistostromal ophiolite complex was named as Karayaprak Mixture [6]. Ophiolites are generally located on the complex with a tectonic contact (Figure 5). Munzur Limestone, on the other hand, is mainly represented by platform type carbonates and is located under the Erzincan Nappe [7]. It begins with algal limestone of Upper Triassic - Lower Jurassic age, continues with ophiolite limestone, algal-foraminiferous limestone and occasionally flintlock limestone. On the limestones in the upper levels of this unit, flintlock pelagic limestone of Turonian-Campanian age is overlaid with a harmonious and sharp contact. The units of Middle Eocene-Quaternary age representing the cover overlie the tectonic units with an angular unconformity. The clastic succession of Middle Eocene age passes to the upper levels in conformity with first volcano-sedimentary and then massive volcanic.





Figure 4: Location map of the Erzincan Plain and surroundings

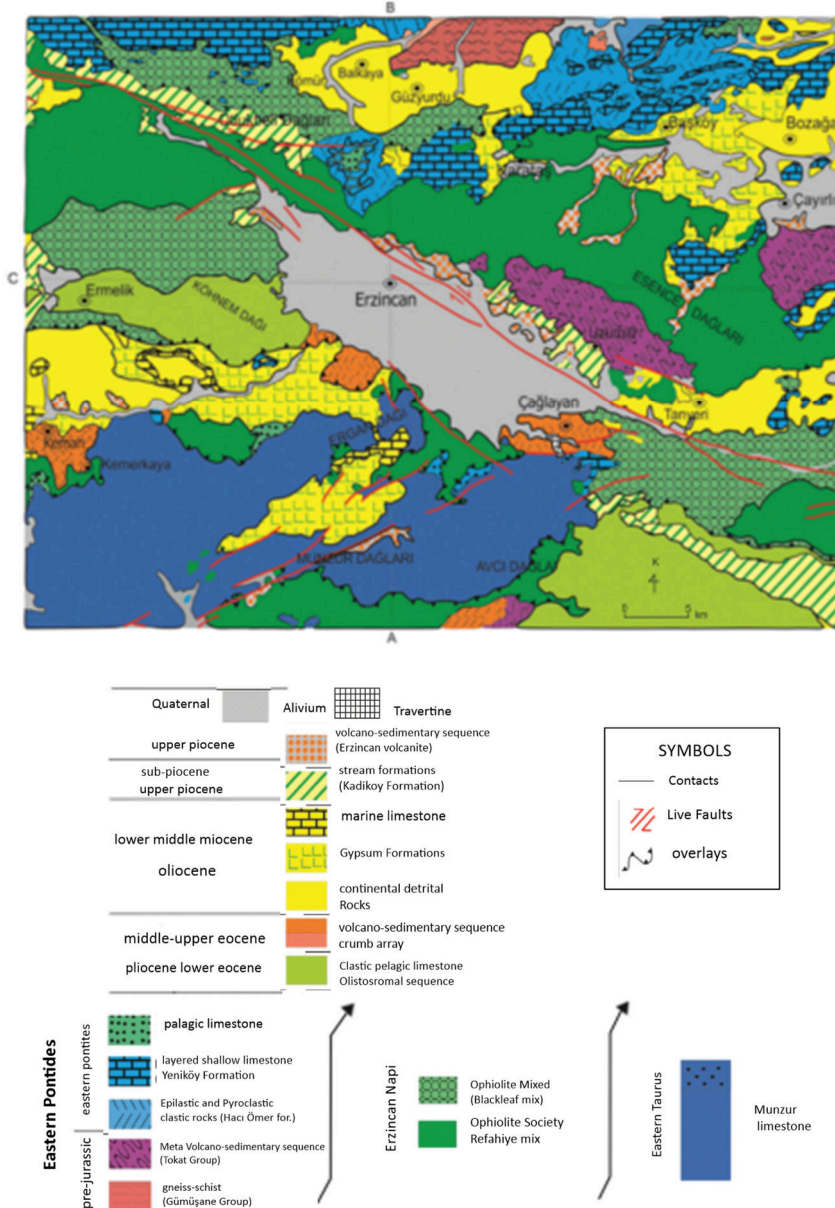


Figure 5: The geology of the region [8 modified]

Terrestrial and shallow marine succession of Oligocene-Lower Miocene age mainly consists of evaporites and all the older units come on the rocks with an angular unconformity. These units offer a transitional structure in the lateral and vertical directions. A large part of the Erzincan Plain is made up of units of Quaternary age. Alluvial fans common in the basin represent a good aquifer for groundwater. Their thickness is 50-150 m. Ophiolites are located at the base of this alluvial material, which is in between [8].

Tectonic

The main faults characterizing the Erzincan Plain and the segments of the North Anatolian Fault Zone limiting the basin from the north have been studied in detail [8, 9, 10]. The Erzincan Basin and the North Anatolian Fault Zone in its vicinity are divided into three segments and two of these segments are observed in and around the basin. The eastern segment is approximately 75 km and is located in the N1100E direction between Yedisu-Tanyeri (Avcılar). The second segment, on the other hand, forms the northern border of the basin and is approximately 60 km long and strikes N1250E [10]. In order to reveal the tectonic and seismicity of the region, it would be beneficial to first examine the location of the structures belonging to the regional neotectonic period. The North Anatolian Fault (NAF) borders the Erzincan Plain from the north and has a right-lateral strike-slip fault character. In the south of Erzincan, there is the Ovacık Fault zone (OF), which consists of left-sided, northeast-southwest trending and parallel faults. All of these faults were formed by a compression in the north-south direction. When this system is considered in macro terms, it gives the impression that the Erzincan Plain was opened with the westward movement of the Anatolian plate, just like Karlıova. Although the normal faults in the study area are widely observed at the basin edges, they are also observed in the younger unit forming the basin fill. These faults are generally SE-NW and E-W trending faults, as well as small scale faults with approximately N-S trending in some parts [11]. As a result, it can be accepted that the Erzincan Plain is an intra-continental basin developed under the control of the NAF (that is, a right-lateral strike-slip regime) and other tectonic elements in its vicinity, and it continues to form under the control of a N-S-trending compression today. In the last 1000 years, more than 10 earthquakes with an intensity greater than 7 have occurred in the Erzincan region [12].

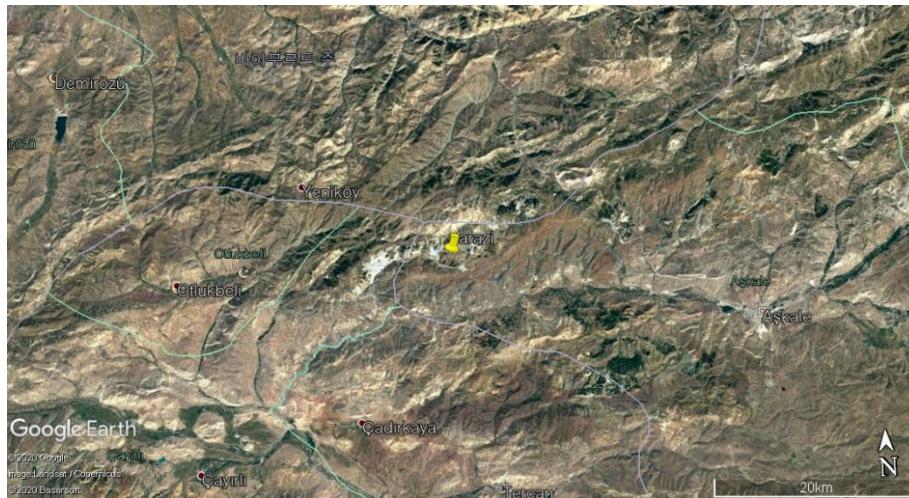


Figure 6: The study area of Erzincan-Kop mountain region

Geophysical Studies

In September 1998, Birlik Madencilik A.Ş. Geophysical studies were carried out at 485 stations for the purpose of Chrome (Figure 6). Gravity measurements were measured with a La Coste-Romberg D model micro gravimeter. Birlik Madencilik A.S. proposed site; In the 20mx 20m grid, its perimeter was enlarged in 20mx40m and 40mx40m grids in accordance with the purpose. Gravity measurements were made at 485 stations in the field. Gravity measurements were taken with a La Coste-Romberg D model micro gravimeter (Figure 7). The CNN method was applied to the Bouguer anomaly map obtained in the Erzincan Kop region and the map given in figure 8 was obtained.



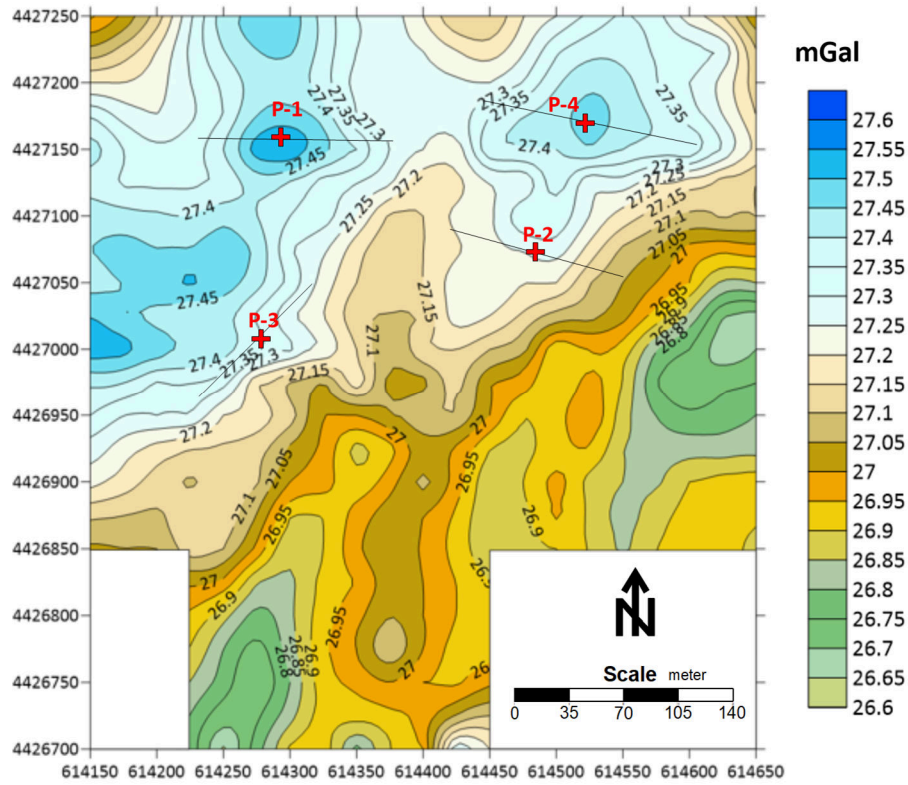


Figure 7: Bouguer anomaly map obtained in the region

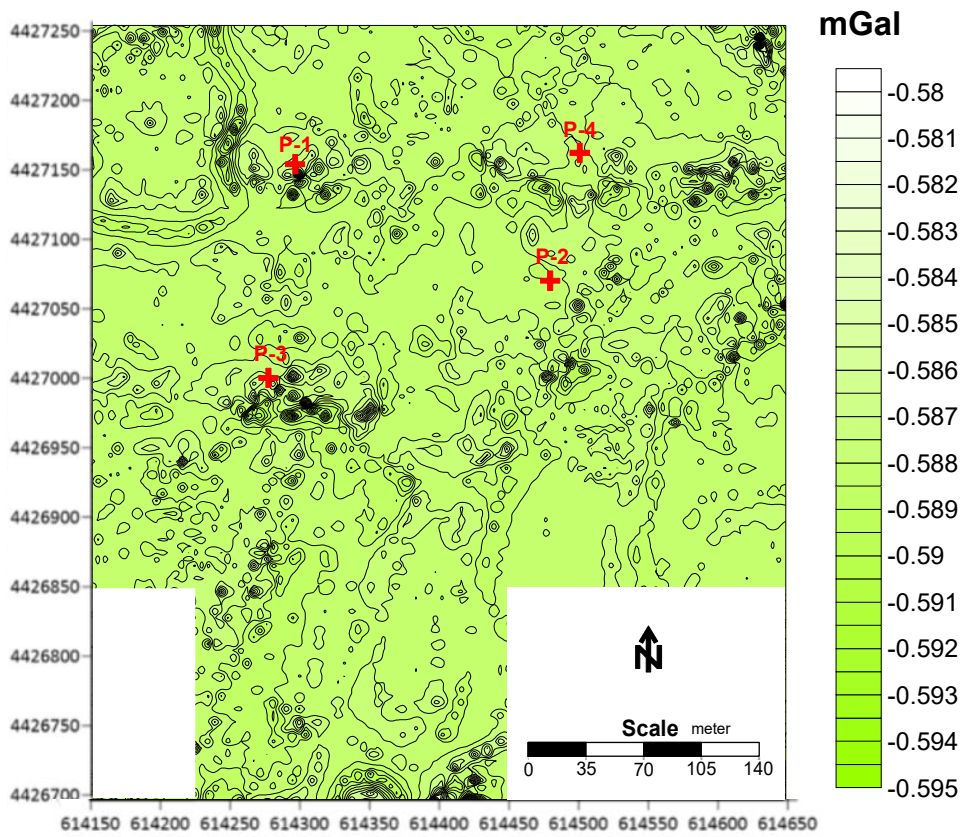


Figure 8: CNN output of the Bouguer anomaly map

Conclusion

The CNN output of the gravity Bouguer map and the Bouguer anomaly map were examined together. In the Gravity Bouguer anomaly map, cross-sections were taken at the places where positive anomalies No. P1, P2, P3, P4 were found and these sections are given in Figure 9. Drillings were made at P-1, P-2, P-3 and P-4 points where the Bouguer anomaly map gave anomaly. In the P-1 drill, there is Dunite with pyroxene between 45-51 meters and Dunite between 60-63 meters. Increasingly, distamine chromite was detected in the faulted parts of the fractured and faulted dunite between 51-66m. Dunite with proxin was found between 15-18 meters and between 33-36 meters in drilling numbered P-2. Dunite was encountered at 46-49 meters in the drilling no. P-3. Proxene dunite was observed between 49-53 meters. Again, at this drilling point, 1 cm of chromite ore was encountered in the form of scattering in the pyroxene banded dunite between 9-15 m and in the pyroxene bands at 48-50 m. Dunite was detected between 47-60 meters at the drilling site P-4. Positive anomalies are observed due to the density difference between the Chromite Ore and other host rocks in the drillings made in the areas where positive anomalies are found on the Bouguer anomaly map. Density analyzes of the cores taken from the drillings were made in the laboratories of the MTA General Directorate, and susceptibility measurements of the same samples were also made. Although there is a density difference between the chromite ore and other rocks, no gravity anomaly corresponding to the Chromite ore, which may form a large deposit, could not be detected in the study area.

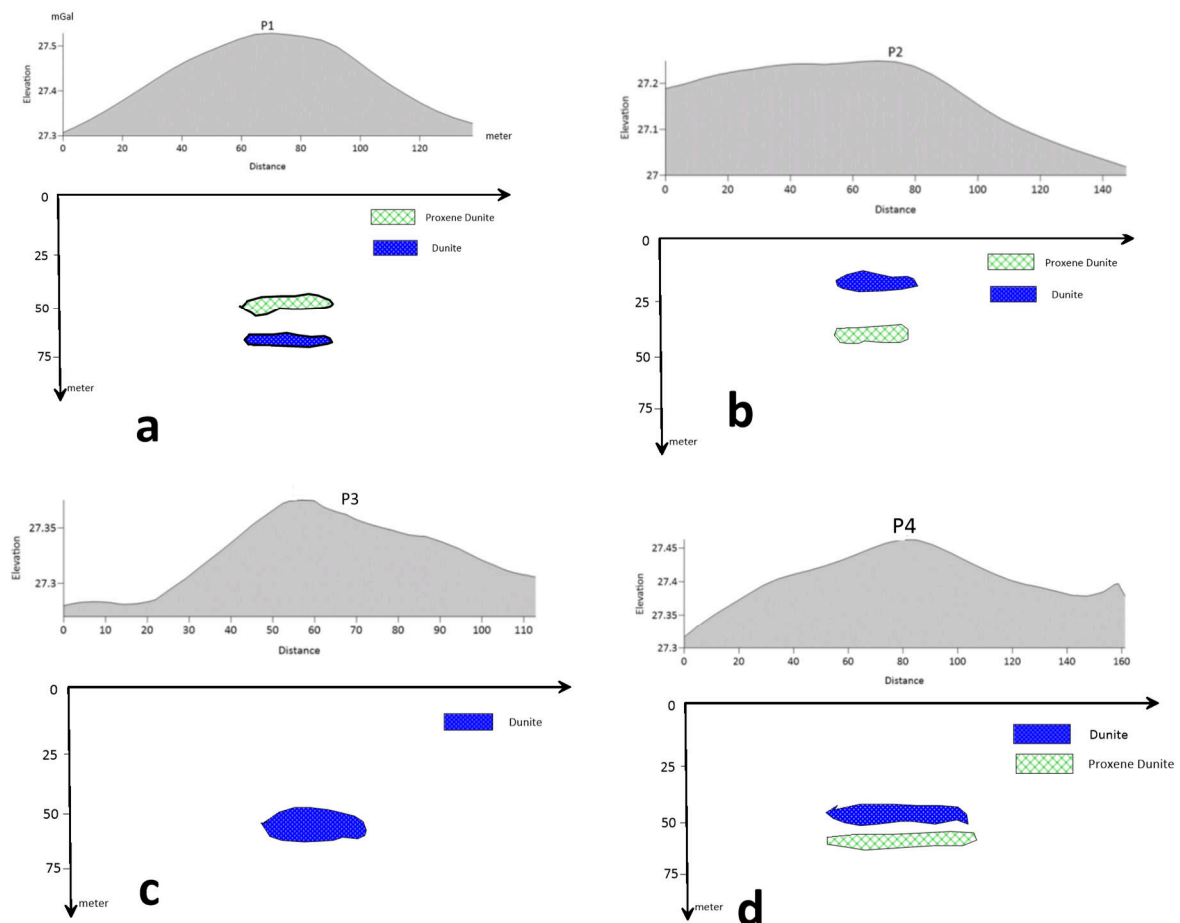


Figure 9: Model studies based on a) P-1, b) P-2, c) P-3, d) P-4 profiles obtained from the Bouguer anomaly map

When we look at the CNN outputs, it is thought that it would be beneficial to drill in areas where anomalies are intense, just south of the P-1 drilling site. Drills can be drilled on the south and southeast sides of the P-3 and P-4 drilling sites in the same way, where anomalies are intense.



Acknowledgement

I would like to thank all my friends and Mineral Research and Exploration Institute (MTA) employees who contributed to the removal of gravity anomalies and drillings.

References

- [1]. Sabri K., 2018, Türkiye’de Kromit üretiminde cevher zenginleştirmenin 100. Yılı. TMMOB Maden Mühendisleri Odası Adana Şubesi, Krom çalıştay, 13. Ekim 2018 Adana.
- [2]. Özkoçak, O., 1972, Alpin Tipindeki Kromit Yataklarının Özellikleri ve Araştırılması, TMMOB Maden Mühendislik Odası Madencilik dergisi, 11, 2, 25-38.
- [3]. Chua, L.O. and Yang, L. 1988, Cellular Neural Networks: Theory, IEEE Trans. On Circuits and Systems, 35, 1257-1272.
- [4]. Albora A. M., Uçan O. N., Özmen A. and Tulay Ö., (2001a), Evaluation of Sivas-Divrigi Region Akdag Iron Ore Deposits Using Cellular Neural Network, Journal of Applied Geophysics, 46, 129-142.
- [5]. Albora A.M., Özmen A., Uçan O.M., (2001b), Residual Separation of Magnetic Fields Using a Cellular Neural Network Approach, Pure and Applied Geophysics, vol.158, pp.1797-1818, 2001.
- [6]. Yılmaz, A. (1985), Yukarı Kelkit Çayı ile Munzur Dağları arasının temel jeoloji özellikleri ve yapısal evrimi: Journal of Geological Engineering, 28/2, 79-92.
- [7]. Özgül, N. 1981, Munzur dağlarının jeolojisi. MTA Derleme Rapor No, 6995, Ankara, 136.
- [8]. Boz, D. and Yılmaz, A. (2020), An Approach to the Planning and Environmental Geology of Erzincan Plain and its Surroundings, Journal of Geological Engineering 44 225-254.
- [9]. Arpat, E., Şaroğlu, F., 1975. Türkiye’de bazı önemli genç tektonik olaylar. Journal of Geological Engineering, 18/1, 91-101.
- [10]. Barka, A. A., Gülen, L., 1989. New constraints on the age and total offset of the North Anatolian Fault Zone: implications for tectonics of the Eastern Mediterranean Region. METU Journal of Pure Applied Science, 21, 39-63.
- [11]. Akpınar, Z., (2010). Erzincan havzasının tektonik gelişiminin Paleomanyetik yöntemlerle analizi. Cumhuriyet Üniversitesi Fen Bilimleri Enstitüsü, Doktora tezi, Sivas, 170s.
- [12]. Boz, D., 2015. Erzincan İli ve Dolayının Çevre Jeolojisi ve Geleceğe Yönelik Planlaması. TC Cumhuriyet Üniversitesi, Fen Bilimleri Enstitüsü, Yüksek lisans tezi (Yayımlanmamış), Sivas, 109 s.

